Effects of N-doping concentration on the electronic structure and optical properties of N-doped β-Ga_2O_3*

Zhang Li-Ying(张丽英), Yan Jin-Liang(闫金良)†, Zhang Yi-Jun(张易军), and Li Ting(李 厅)

School of Physics, Ludong University, Yantai 264025, *China*

(Received 15 August 2011; revised manuscript received 13 December 2011)

The electronic structures and the optical properties of N-doped β-Ga_2O_3 with different N-doping concentrations are studied using the first-principles method. We find that the N substituting O(1) atom is the most stable structure for the smallest formation energy. After N-doping, the charge density distribution significantly changes, and the acceptor impurity level is introduced above the valence band and intersects with the Fermi level. The impurity absorption edges appear to shift toward longer wavelengths with an increase in N-doping concentration. The complex refractive index shows metallic characteristics in the N-doped β-Ga_2O_3.

Keywords: first-principles, p-type β-Ga_2O_3, N-doped, electronic structure, optical properties

PACS: 71.20.–b, 71.20.Nr, 78.20.–e, 71.15.Ap **DOI:** 10.1088/1674-1056/21/6/067102

1. Introduction

β-Ga_2O_3 is an important wide band gap (about 4.8 eV) compound which has excellent thermal and chemical stability.[1,2] It has drawn significant attention from scientists because of its potential applications in different fields such as luminescent materials,[3,4] including flat panel displays, solar energy conversion devices, optical limiters for deep ultraviolet radiation,[5,6] high-temperature stable gas sensors,[7,8] antireflection coating on GaAs,[9,10] passivation coating,[11,12] and so on. It can also be used as a transparent conductive electrode of optoelectronic devices.[13] Additionally, the magnetism of the conduction electron spin of β-Ga_2O_3 exhibits an original memory effect with a wide range of temperatures from 4 K to room temperature.[14] On the other hand, syntheses one-dimensional gallium–oxide structures like nano-rods, belts, and wires.[15,16]

For the application of transparent conductive oxide, the control of conductivity and the substitute doping are undoubtedly important. But the conductivity of intrinsic β-Ga_2O_3 is too poor to meet the requirements of most applications. The introduction of the shallow acceptor levels into the wide band-gap semiconductor to form holes in the valence band is more difficult than in narrow gap oxides. This greatly reduces the number of candidate materials for p-type deep-UV transparent conductive oxide (TCO).[17,18] So p-type doping has still been a major obstacle for the device application. Selecting the appropriate doping elements to improve the electrical and optical properties is very important. The negative trivalent nitrogen ion is chosen as the dopant, for the ionic radius of the N^{3-} is close to O^{2-} and the N^{3-} prefers to substitute O^{2-} sites.[19] Thus, we can expect the introduction of the N^{3-} ion to form shallow acceptor levels. Recently, a few experimental studies have been carried out to explore the properties of N-doped β-Ga_2O_3. Liu *et al.*[20] used the CVD method to prepare a N-doped β-Ga_2O_3 nanowire which had a p-type electrical conductivity. To the best of our knowledge, there is no theoretical calculation work on the electronic structures and optical properties in different concentrations of N-doped β-Ga_2O_3.

2. Details of calculations

All the calculations were completed by the CASTEP[21,22] software package in Materials Studio (MS) 5.0 software. It is a quantum mechanics program *ab initio* simulation package[23] based on the density functional theory (DFT). Making use of the plane wave pseudo-potential technology of general energy, where an ion potential is replaced by ultra-soft pseudo-potential, electronic wave function is unfolded

*Project supported by the National Natural Science Foundation of China (Grant No. 10974077), the Natural Science Foundation of Shandong Province, China (Grant No. 2009ZRB01702), and the Shandong Provincial Higher Educational Science and Technology Program, China (Grant No. J10LA08).

†Corresponding author. E-mail: yanjinliang@yahoo.cn

© 2012 Chinese Physical Society and IOP Publishing Ltd

with plane wave base groups.[24,25] The generalized gradient approximation (GGA) in the Perdew, Burke, and Ernzerhof (PBE) scheme is adopted for describing the exchange–correlation interactions.[26−29]

Basic parameters were chosen as follows: kinetic energy cut-off was 340 eV; SCF tolerance was 1.0×10^{-6} eV·atm^{-1} (1 atm=1.01325 × 10^5 Pa); the special K points of 2×4×2 monkorst-parks scheme are summed in all the Brillouin zone in reciprocal space;[30−32] the maximum displacement is 0.001 Å (1 Å=0.1 nm); the force per atom is lower than 0.03 eV·nm^{-1}; the tolerance deviation and stress deviation are 0.02 nm and 0.05 Gpa respectively. The electronic states of $2s^22p^4$, $3d^{10}4s^24p^1$, and $2s^22p^3$ are considered as the valence states for O, Ga, and N respectively.

3. Results and discussion

3.1. Formation energies and structural properties

In this paper, the 1×2×2 supercell β-Ga_2O_3 has two different Ga sites, denoted as Ga(1) and Ga(2), and three different O sites denoted as O(1), O(2), and O(3). Throughout this paper, we identify the atomic positions according to Ref. [28]. The β-Ga_2O_3 belongs to space group $C2/m$ with the two-fold rotation axis b. The Ga atom is surrounded by O atoms in either tetrahedral Ga(1) or octahedral Ga(2) coordination site.

Table 1. Formation energies of N-doped β-Ga_2O_3 compounds with different N-doping concentrations.

Formation energies	$E_1^{\rm f}$	$E_2^{\rm f}$	$E_3^{\rm f}$
$E^{\rm f}[N_{\rm O}^0]$/eV	–0.394	–0.115	–0.163

The formation energy of a defect or impurity N in charge state $q=0$ is defined as[33]

$$E^{\rm f}[N_{\rm O}^0] = E_{\rm tot}[N_{\rm O}^0] - E_{\rm tot}[{\rm Ga_2O_3, bulk}] - \mu_{\rm N_2} + \mu_{\rm O_2} - E_{\rm corr}, \quad (1)$$

where $E_{\rm tot}[N_{\rm O}^0]$ is the total energy derived from a supercell calculation with impurity or defect N in the cell; $E_{\rm tot}[{\rm Ga_2O_3, bulk}]$ is the total energy for the equivalent supercell containing only bulk Ga_2O_3; $\mu_{\rm N_2}$ and $\mu_{\rm O_2}$ are the corresponding chemical potentials of solid nitrogen molecules and solid oxygen molecules respectively; the correction term $E_{\rm corr}$ can be obtained from the energy difference between the highest occupied states at the G point and the special k point. The calculated formation energies of N-doped β-Ga_2O_3 compounds with different N-doping concentrations are shown in Table 1. The $E_1^{\rm f}$, $E_2^{\rm f}$, $E_3^{\rm f}$ represent the formation energies when O(1), O(2), and O(3) atoms are substituted by N atoms respectively. The smallest formation energy is $E_1^{\rm f}$, which indicates that the N substituting O(1) atom is the most stable structure. So we mainly study the N substituting O(1) atom in this work.

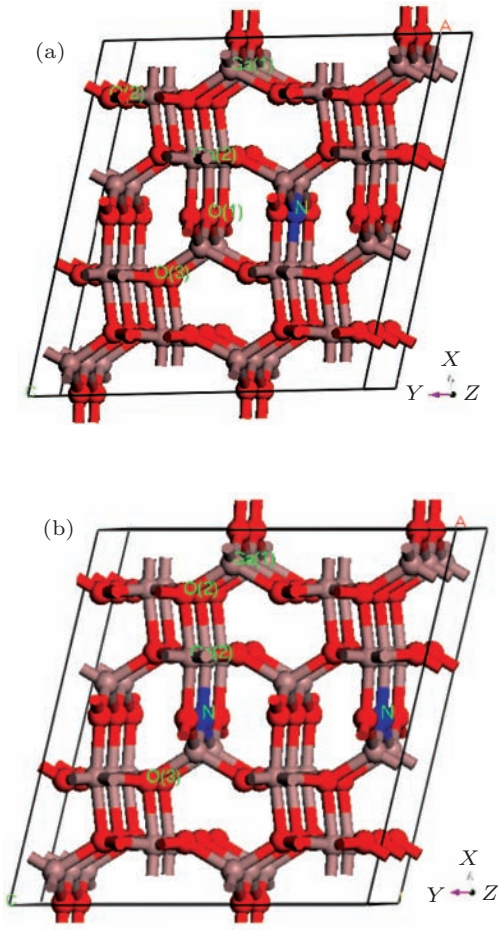


Fig. 1. (colour online) Crystal structures of (a) 1 at% N-doped β-Ga_2O_3 and (b) 2 at% N-doped β-Ga_2O_3.

The two 1×2×2 supercells of N-doped β-Ga_2O_3 with 1 at% and 2 at% doping concentrations are shown in Figs. 1(a) and 1(b) respectively. The geometry is optimized using the Broyden–Fletcher–Goldfarb-Shanno minimization algorithm. The equilibrium structure is obtained after the cell geometry and volume are fully relaxed by minimizing the total energy and forces. The calculated equilibrium lattice constants of intrinsic and N-doped β-Ga_2O_3 are shown in Table 2. With the increase of the N-doping concentration, the lattice constants a, b and the original cell volume V increase, but the lattice constant c decreases. The ionic radius of O^{2-} ion (0.132 nm) is smaller than the N^{3-} ion radius (0.146 nm), so the original cell volume increases after the O atom is substituted by the N atom.

Table 2. Intrinsic and N-doped β-Ga_2O_3 lattice constants.

	a/Å	b/Å	c/Å	α	β	γ	V/Å^3
122-reference	12.230	6.080	11.600	90.000	103.700	90.000	838.017
122-intrinsic-GGA	12.526	6.198	11.820	90.000	103.674	90.000	891.665
1 at% N-doped-GGA	12.567	6.207	11.796	90.000	103.622	90.000	893.983
2 at% N-doped-GGA	12.583	6.217	11.780	90.000	103.619	90.000	895.690

3.2. Charge density

Figures 2 and 3 show the contour plots of the difference charge density on the (010) plane for 1 at% and 2 at% N-doped β-Ga_2O_3 compounds. The density difference distribution is used to analyse the bonding characteristics of the crystal. The ionic or covalent character in β-Ga_2O_3 is a controversial topic and is important information in order to interpret the transport properties of the material. The covalent character can be clearly seen between the Ga–O bonds in intrinsic β-Ga_2O_3. The introduction of the N impurity causes the charge density distribution to significantly change.

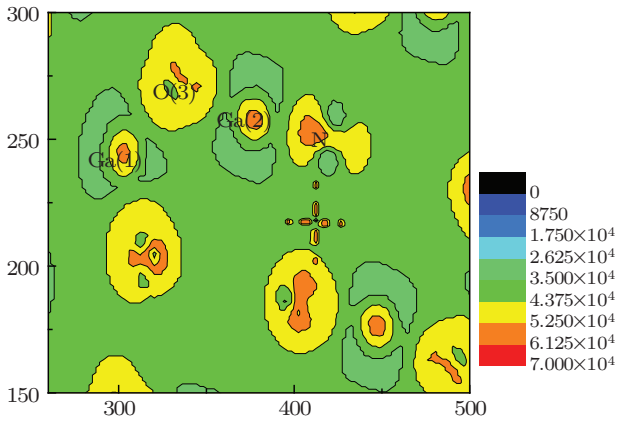


Fig. 2. (colour online) Contour map of difference charge density on the (010) plane of 1 at% N-doped β-Ga_2O_3.

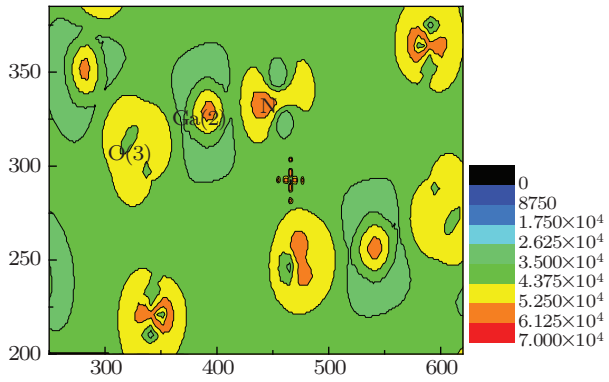


Fig. 3. (colour online) Contour map of difference charge density on the (010) plane of 2 at% N-doped β-Ga_2O_3.

The interaction of charge density between the N atom and Ga(2) atom is weakened. It results from the fact that the electronegative value between N(3.04) and Ga(1.81) atoms is less than that between O(3.44) and Ga(1.81) atoms. The N-Ga(2) bond trends to break and release electrons, thereby forming holes around the impurity level.

3.3. Band structures and density of states

Figure 4 shows the band structure of 1 at% N-doped β-Ga_2O_3 along the high symmetry points across the Brillouin zone. The Fermi level is sited at zero-point of energy. The corresponding total density of states (TDOS) and partial densities of states (PDOSs) are shown in Fig. 5.

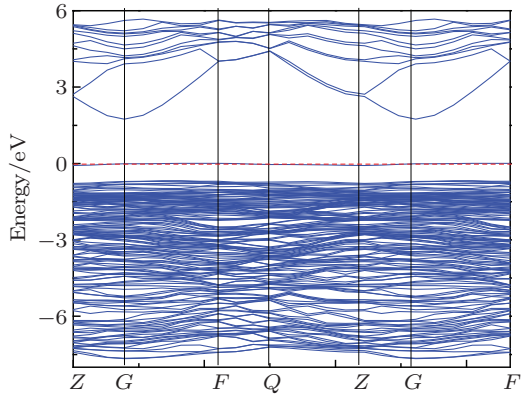


Fig. 4. (colour online) Band structure of 1 at% N-doped β-Ga_2O_3.

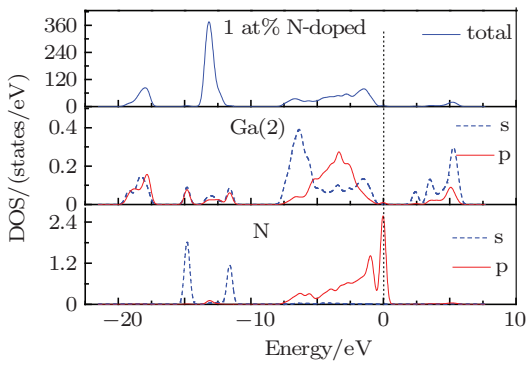


Fig. 5. (colour online) Total density of states and partial densities of states for 1 at% N-doped β-Ga_2O_3.

The valence band maximum (VBM) and the conduct band minimum (CBM) are located at the same

G point.[34,35] The acceptor impurity level lies above the valence band (about 0.7 eV at the Z point) and intersects with the Fermi level. It acts as acceptor of electrons excited from the valence band to turn the N-doped β-Ga_2O_3 into a p-type semiconductor. But the acceptor impurity level is too deep to be thermally excited at room temperature. That can be used to explain why we cannot prepare a high p-type conductive N-doped β-Ga_2O_3 in experiments.

There are three valence bands. The upper part of the valence bands is formed mainly by the bonding state of the Ga 4s, 4p and N 2p orbits. The characteristics of β-Ga_2O_3 are determined mainly by the top of valence band and the bottom of the conduction band. So we will not discuss the middle valence band or the lower valence band. The bottom of conduction band is located between 1.73 eV and 5.68 eV, which is mainly formed by the Ga 4s and 4p states, and the N 2p states also have a minor contribution. Figure 6 shows the band structure of 2 at% N-doped β-Ga_2O_3. The intersection part between the acceptor impurity level and the Fermi level is strengthened compared with 1 at% N-doped β-Ga_2O_3. However, the energy gap between the acceptor impurity level and the top of the valence band is 0.6 eV at the Z point, which is 0.1 eV smaller than that in the case of 1 at% N-doped β-Ga_2O_3. It indicates that the P-type effect is enhanced. Figure 7 shows the total density of states and partial densities of states for 2 at% N-doped β-Ga_2O_3 respectively. The top of the valence band and the bottom of the conduction band are composed mainly of the N 2p states and the Ga 4s and 4p states respectively. The N 2p state and Ga 4s and 4p states display extensive overlap, which indicates the interactions between N and Ga atoms. The characteristic peak of the valance band is located around 12 eV which is weaker than that in the case of 1 at% N-doped β-Ga_2O_3.

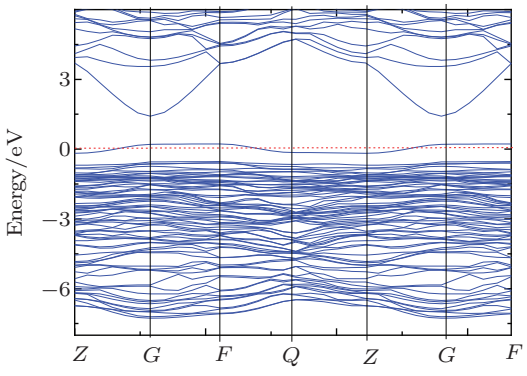


Fig. 6. (colour online) Band structure of 2 at% N-doped β-Ga_2O_3.

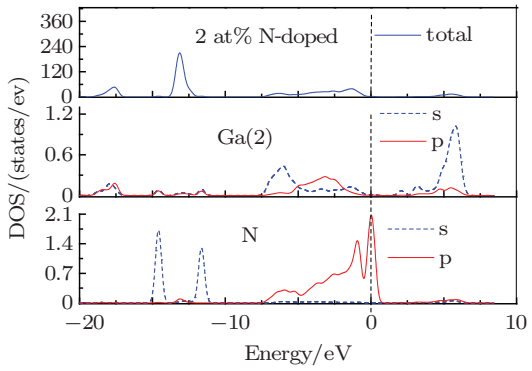


Fig. 7. (colour online) Total density of states and partial densities of states for 2 at% N-doped β-Ga_2O_3.

3.4. Optical properties

The dielectric function can be explained by the band-to-band transition, and the real part $\varepsilon_1(\omega)$ (ω is the light frequency) of the dielectric function can be derived from the imagining part $\varepsilon_2(\omega)$ using the Kramers–Kronig dispersion equation.

The real part $\varepsilon_1(\omega)$ and the imaginary part $\varepsilon_2(\omega)$ components for both 1 at% and 2 at% N-doped β-Ga_2O_3 are plotted in Figs. 8 and 9 in a wide energy range of 0–25 eV. The anisotropies in the dynamic dielectric function are observed in 1 at% and 2 at% N-doped β-Ga_2O_3 compounds. The ε_{zz} is distinguished from ε_{xx} and ε_{yy}, which are related by the chain-type structure along the b axis. The major peaks (peak 2) are located at 7.1 eV for 1 at% N-doped β-Ga_2O_3 and 6.8 eV for 2 at% N-doped β-Ga_2O_3, which are attributed to the inter-bands transition from the excitation of N-2p electrons in the valence band to the Ga-4s conduction band. There are weak peaks (peak 1) appear at 1.73 eV and 1.22 eV for 1 at% and 2 at% N-doped β-Ga_2O_3 respectively, which represent the transition from the acceptor impurity levels to the bottom of conduction band.

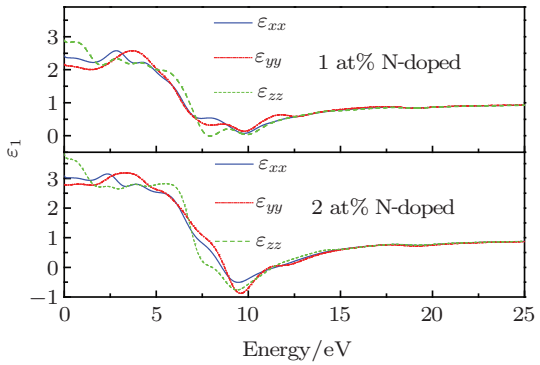


Fig. 8. (colour online) Real parts of the dielectric functions for 1 at% and 2 at% N-doped β-Ga_2O_3 compounds.

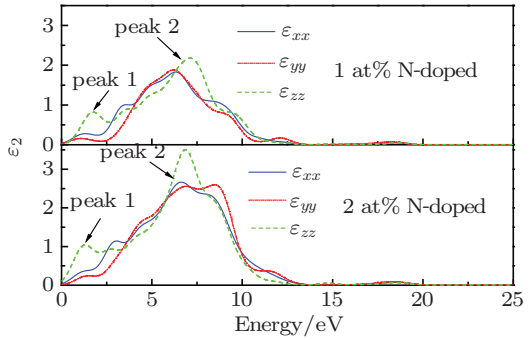


Fig. 9. (colour online) Imaginary parts of the dielectric functions for 1 at% and 2 at% N-dope β-Ga_2O_3 compounds.

The absorption spectra of 1 at% and 2 at% N-doped β-Ga_2O_3 are shown in Fig. 10. The impurity absorption edges appear in N-doped β-Ga_2O_3, which result from the inter-band transition from the N acceptor impurity levels to the conduction band. In addition, the impurity absorption edges are intensified and shifted toward longer wavelength with the increase of N-doped concentration.

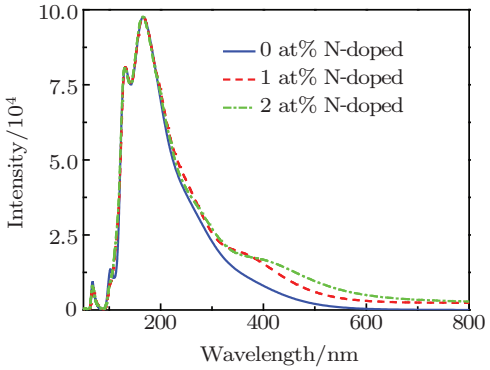


Fig. 10. (colour online) Absorption spectra for 1 at% and 2 at% N-doped β-Ga_2O_3 compounds.

Figure 11 shows the complex refractive indexes of 1 at% and 2 at% N-doped β-Ga_2O_3 compounds. The complex refractive index $\tilde{n}$ is determined by

$$\tilde{n} = n + \mathrm{i}\,\kappa, \tag{2}$$

where n and κ are the refractive index and extinction coefficient respectively, which can be expressed as

$$n^2 - \kappa^2 = \varepsilon_1, \tag{3}$$

$$2n\kappa = \varepsilon_2. \tag{4}$$

The values of the refractive index n_0 are 1.58 and 1.80 for 1 at% and 2 at% N-doped β-Ga_2O_3 respectively. The κ is lager than n in the energy range of 8.5 eV–11.2 eV for 2 at% N-doped β-Ga_2O_3, which indicates that the light cannot transmit in these photon energy region and exhibits metal reflection characteristics. It is consistent with the first-principles calculation of electronic structure and optical properties of In_2O_3 by Zhang *et al.*[36]

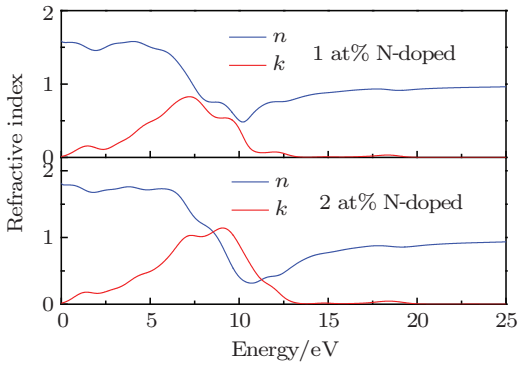


Fig. 11. (colour online) Refractive indexes for 1 at% and 2 at% N-doped β-Ga_2O_3 compounds.

4. Conclusions

The electronic structures and the optical properties of N-doped β-Ga_2O_3 are studied using first-principles calculations. With the increase of N-doping concentration, the lattice constants are changed significantly and the interaction between the N–Ga(2) is weakened. The acceptor impurity levels are introduced above the valence band and intersect with the Fermi levels of N-doped β-Ga_2O_3. The anisotropic optical properties are observed. The impurity absorption edges shift toward a longer wavelength and the metal reflective characteristics are observed in 8.5 eV–11.2 eV for the 2 at% N-doped β-Ga_2O_3. All the calculation results indicate that N is a very promising p-type doping source to obtain the p-type β-Ga_2O_3 compound.

References

[1] Sinha G, Ganguli D and Chaudhuri S 2006 *J. Phys.: Condens. Matter* **18** 11167
[2] Tippins H H 1965 *Phys. Rev.* **140** A316
[3] Binet L and Gourier D 1998 *J. Phys.: Chem. Solids* **59** 1241
[4] Hao J H and Cocivera M 2002 *J. Phys.* D **35** 433
[5] Litimeina F, Racheda D and Khenatab R 2009 *J Alloys Compd.* **205** 126
[6] Ueda N, Hosono H, Waseda R and Kawazoe H 1997 *Appl. Phys. Lett.* **71** 933
[7] Ogita M, Saika N, Nakanishi Y and Hatanaka Y 1999 *Appl. Surf. Sci.* **142** 188
[8] Deng B, Sun H Q, Guo Z Y and Gao X Q 2010 *Acta Phys. Sin.* **59** 1212 (in Chinese)
[9] Rebien M, Herion W, Hong M, Mannaerts J P and Fleischer M 2002 *Appl. Phys. Lett.* **81** 250

[10] Shan F K, Liu G X, Lee W J, Lee G H, Kim I S and Shin B C 2005 *J. Appl. Phys.* **98** 023504
[11] Passlacki M, Schubert E F, Hobson W S and Hong M 1995 *J. Appl. Phys.* **77** 686
[12] Zheng L, Jiang C B, Shang J X and Xu H B 2009 *Chin. Phys.* B **18** 1647
[13] Edwards D D, Mason T O, Goutenoire F and Poeppelmeier K R 1997 *Appl. Phys. Lett.* **70** 1706
[14] Hajnal Z, Miró J, Kiss G, Réti F, Deák P, Herndon R C and Kuperberg J M 1999 *J. Appl. Phys.* **86** 3792
[15] Aubay E and Gourier D 1993 *Phys. Rev.* B **47** 15023
[16] Rao R, Rao A M, Xu B, Dong J, Sharma S and Sunkara M K 2005 *J. Appl. Phys.* **98** 094312
[17] Kim H W and Kim N H 2005 *J. Mater. Sci.* **40** 4703
[18] Huang G Y, Wang C Y and Wang J T 2010 *Chin. Phys.* B **19** 013101
[19] Zhang Y J, Yan J L and Zhao G 2010 *Physica* B **405** 3899
[20] Liu L L, Li M K and Yu D Q 2010 *J. Appl. Phys.* A **98** 831
[21] Medvedeva J E and Chaminda L H 2010 *Phys. Rev.* B **81** 125116
[22] Segall A M D, Lindan P L D and Probert M J 2002 *J. Phys.: Condens. Matter* **14** 2717
[23] Feng J, Xiao B, Chen J C and Zhou C J 2009 *Solid State Sci.* **11** 259
[24] Xu B, Cheng Z Z, Yi L and Cheng Z 2008 *Chin. Phys.* B **17** 3798
[25] Perdew J P, Burke K and Ernzerhof M 1996 *Phys. Rev. Lett.* **77** 3865
[26] Zhang Y J, Yan J L, Zhao G and Xie W F 2011 *Acta Phys. Sin.* **60** 037103 (in Chinese)
[27] Vanderbilt D 1990 *Phys. Rev.* B **41** 7892
[28] Monkhorst H J and Pack J D 1976 *Phys. Rev.* B **13** 5188
[29] Fischer T H and Alml J 1992 *J. Phys. Chem.* **96** 9768
[30] Medvedeva J E, Teasley E N and Hoffman M D 2007 *Phys. Rev.* B **76** 155107
[31] Yu D L, Chen Y H, Cao Y J and Zhang C R 2010 *Acta Phys. Sin.* **59** 1991 (in Chinese)
[32] Yamaga M, Villora E G, Shimamura K, Ichinose N and Honda M 2003 *Phys. Rev.* B **68** 155207
[33] Chris G, Van de Wallea and Jorg Neugebauer 2004 *Appl. Phys. Rev.* **95** 3582
[34] Hu C E, Zeng Z Y, Cheng Y, Chen X and Cai L C 2008 *Chin. Phys.* B **17** 3867
[35] Zhang F Y, You J Q, Zeng Z and Zhong G H 2007 *Chin. Phys.* **16** 3815
[36] Zhang F C, Zhang Z Y and Zhang W H 2008 *Chem. J.* **66** 1863 (in Chinese)